

Electronic Supplementary Materials

*Fluorinated tolane-based fluorophores bearing a branched flexible unit
with aggregation-induced emission enhancement characteristics*

Shigeyuki Yamada,* Masaya Sato, Eiji Uto, Mitsuki Kataoka,
Masato Morita and Tsutomu Konno

Faculty of Molecular Chemistry and Engineering, Kyoto Institute of Technology,
Matsugasaki, Sakyo-ku, Kyoto 606-8585, Japan

*Correspondence: syamada@kit.ac.jp; Tel: +81-75-724-7517

Table of Contents:

1. Experimental	••••••••••	S-2
2. NMR Spectra	••••••••••	S-5
3. X-ray crystallographic analysis	••••••••••	S-15
4. DFT Calculation	••••••••••	S-16
Cartesian coordinate	••••••••••	S-18
5. Photophysical Characteristis		
Solution state	••••••••••	S-23
Crystalline state	••••••••••	S-23
AIEE characteristics	••••••••••	S-24

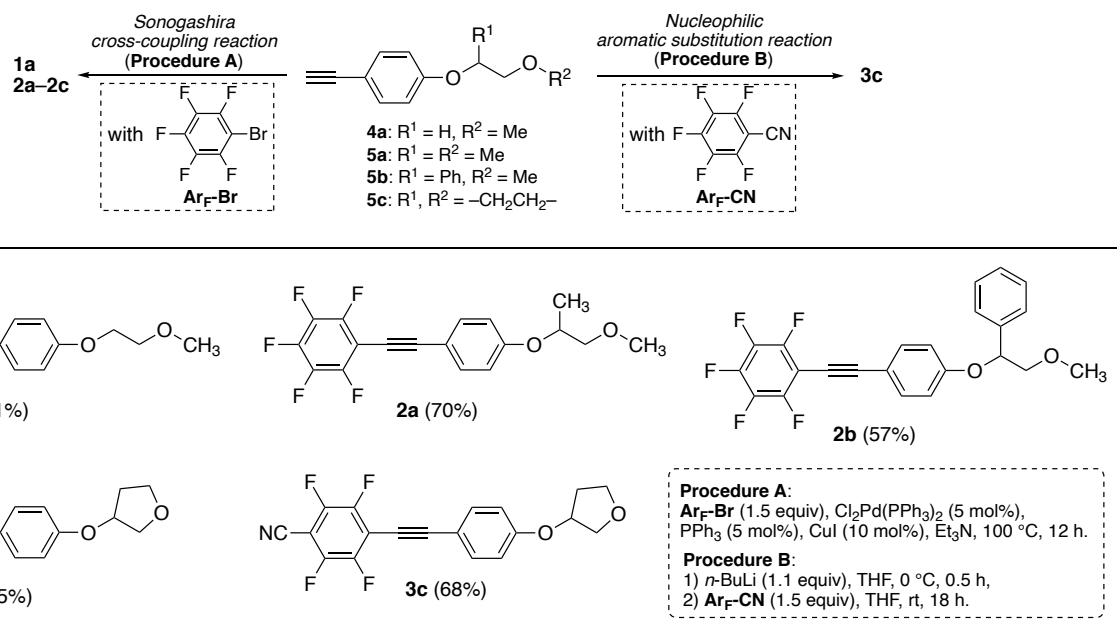
1. Experimental

1.1. General

The progress of the reactions was monitored via thin-layer chromatography (TLC), which was performed on silica gel TLC plates (Merck, Silica gel, 60F₂₅₄; New Jersey, NJ, USA). Column chromatography was performed using silica gel (Fujifilm Wako Pure Chemical Corporation, Wako-gel® 60N, 38–100 µm; Osaka, Japan). ¹H nuclear magnetic resonance (NMR) (400 MHz), ¹³C NMR (100 MHz), and ¹⁹F NMR (376 MHz) spectra were acquired using an AVANCE III 400 NMR spectrometer (Bruker, Rheinstetten, Germany) in chloroform-*d* (CDCl₃) solution. The chemical shifts in ¹H and ¹³C NMR spectra were reported in parts per million (ppm) based on the residual proton or carbon in the NMR solvent. The chemical shift in ¹⁹F NMR spectra were also reported in ppm based on the internal standard, CFCl₃ ($\delta_F = 0$ ppm). Infrared (IR) spectra were recorded using the KBr method using an FTIR-4100 type A spectrometer (JASCO, Tokyo, Japan). IR spectra are reported in wavenumber (cm⁻¹) units. High-resolution mass spectra (HRMS) were recorded on a JMS700MS spectrometer (JEOL, Tokyo, Japan) using the fast atom bombardment (FAB) method.

1.2. Synthesis

Fluorinated tolane-based fluorophores **1a**, **2a–c**, and **3c** were readily synthesized from the corresponding phenylacetylenes **4a** and **5a–c** bearing a suitable flexible unit at the *para*-position. According to the reported literature, the precursors **4a** and **5a–c** were prepared from easily available 2-bromoethanol for **4a** and methyl lactate for **5a**, ethyl mandelate for **5b**, and 3-hydroxytetrahydrofuran for **5c**. The detailed experimental procedures and structural characterization for the synthesis of **1a**, **2a–c**, and **3c** were described below.



Scheme S1. Synthetic procedure of fluorinated tolane-based fluorophores **1a**, **2a–c**, and **3c**.

1.2.1. Typical synthetic procedure for 2,3,4,5,6-pentafluoro-1-[2-[4-(methoxyethoxy)phenyl]ethyn-1-yl]benzene (**1a**) via Pd(0)-catalyzed Sonogashira cross-coupling reaction

In a two-necked round-bottomed flask, equipped with a Teflon®-coated stirrer bar and reflux condenser, was placed 4-methoxyethoxyphenyl acetylene (1.55 g, 5.3 mmol), Cl₂Pd(PPh₃)₂ (0.19 g, 0.3 mmol), PPh₃ (0.07 g, 0.3 mmol), bromopentafluorobenzene (1.6 g, 0.8 mL, 7.6 mmol), and Et₃N (15 mL). To the resultant solution was added CuI (0.10 g, 0.5 mmol) and Et₃N (5 mL), and the whole was stirred at 100 °C overnight. After being stirred at the temperature for 18 h, precipitate formed in the reaction mixture was separated by atmospheric filtration and the filtrate was

poured into saturated aqueous NH₄Cl solution (30 mL). Crude product was extracted with EtOAc (30 mL, three times) and organic layer combined was washed with brine (once). The collected organic layer was dried over anhydrous Na₂SO₄, which was separated by filtration. The filtrate was evaporated in vacuo and subjected to silica-gel column chromatography (eluent: hexane/EtOAc = 15/1), followed by recrystallization from CH₂Cl₂/MeOH (v/v = 1/1), to obtain the title compound in 71% (0.70 g, 1.5 mmol) as a white crystal.

2,3,4,5,6-Pentafluoro-1-[2-{4-(methoxyethoxy)phenyl]ethyn-1-yl]benzene (1a)

Yield: 71%; M.p.: 86.1–87.3 °C; ¹H NMR (CDCl₃): δ 3.45 (s, 3H), 3.76 (t, *J* = 4.8 Hz, 2H), 4.14 (t, *J* = 4.8 Hz, 2H), 6.92 (d, *J* = 8.8 Hz, 2H), 7.49 (d, *J* = 8.8 Hz, 2H); ¹³C NMR (CDCl₃): δ 59.2, 67.4, 70.8, 71.9 (q, *J* = 3.6 Hz), 100.6 (td, *J* = 19.0, 3.6 Hz), 101.8 (q, *J* = 3.0 Hz), 113.8, 114.7, 133.4, 136.0–139.2 (dm, *J* = 240.5 Hz), 139.5–142.6 (dm, *J* = 256.7 Hz), 145.5–148.4 (dm, *J* = 252.2 Hz), 159.9; ¹⁹F NMR (CDCl₃): δ –137.06 (dd, *J* = 21.8, 6.8 Hz, 2F), –154.19 (t, *J* = 21.8 Hz, 1F), –162.68 (ddd, *J* = 21.8, 21.8, 6.8 Hz, 2F); IR (KBr): ν 3002, 2878, 2809, 2223, 1604, 1444, 1415, 1289, 1247, 1122, 1058, 987 cm^{–1}; HRMS: (FAB+) *m/z* [M]⁺ calcd for C₁₇H₁₁F₅O₂: 342.0679; found: 342.0690.

2,3,4,5,6-Pentafluoro-1-[2-{4-(1-methoxy-2-propoxy)phenyl]ethyn-1-yl]benzene (2a)

Yield: 70%; M.p.: 45.5–46.2 °C; ¹H NMR (CDCl₃): δ 1.33 (d, *J* = 6.4 Hz, 3H), 3.41 (s, 3H), 3.45–3.53 (m, 1H), 3.56–3.62 (m, 1H), 4.54–4.64 (m, 1H), 6.92 (d, *J* = 8.8 Hz, 2H), 7.48 (d, *J* = 8.8 Hz, 2H); ¹³C NMR (CDCl₃): δ 16.6, 59.3, 71.8, 73.1, 75.7, 100.6 (td, *J* = 18.3, 3.6 Hz), 101.9 (q, *J* = 2.9 Hz), 113.5, 115.9, 133.4, 136.1–139.2 (dm, *J* = 247.9 Hz), 139.5–142.6 (dm, *J* = 255.9 Hz), 145.4–148.5 (dm, *J* = 248.0 Hz), 159.1; ¹⁹F NMR (CDCl₃): δ –136.9 to –137.2 (m, 2F), –154.0 to –154.4 (m, 1F), –162.5 to –162.8 (m, 2F); IR (KBr): ν 3089, 2982, 2933, 2223, 1602, 1523, 1500, 1446, 1247, 1116, 989, 837 cm^{–1}; HRMS: (FAB+) *m/z* [M]⁺ calcd for C₁₈H₁₃F₅O₂: 356.0836; found: 356.0839.

2,3,4,5,6-Pentafluoro-1-[2-{4-(2-methoxy-1-phenylethoxy)phenyl]ethyn-1-yl]benzene (2b)

Yield: 57%; M.p.: 92.6–93.4 °C; ¹H NMR (CDCl₃): δ 3.48 (s, 3H), 3.68 (dd, *J* = 10.8, 3.2 Hz, 1H), 3.86 (dd, *J* = 10.8, 7.6 Hz, 1H), 5.42 (dd, *J* = 7.6, 3.6 Hz, 1H), 6.93 (d, *J* = 8.8 Hz, 2H), 7.28–7.46 (m, 7H); ¹³C NMR (CDCl₃): δ 59.3, 71.8 (q, *J* = 3.7 Hz), 76.9, 79.6, 100.6 (td, *J* = 18.3, 3.6 Hz), 101.8 (q, *J* = 2.9 Hz), 113.7, 116.1, 126.2, 128.1, 128.6, 133.2, 136.0–139.1 (dm, *J* = 248.6 Hz), 137.8, 139.4–142.6 (dm, *J* = 256.7 Hz), 145.4–148.4 (dm, *J* = 248.0 Hz), 159.0; ¹⁹F NMR (CDCl₃): δ –137.05 (dd, *J* = 21.8, 6.8 Hz, 2F), –154.22 (t, *J* = 21.8 Hz, 1F), –162.66 (td, *J* = 21.8, 21.8, 6.8 Hz, 2F); IR (KBr): ν 3000, 2904, 2829, 2220, 1600, 1497, 1447, 1285, 1243, 1174, 1019, 964, 834 cm^{–1}; HRMS: (FAB+) *m/z* [M]⁺ calcd for C₂₃H₁₅F₅O₂: 418.0992; found: 418.0983.

2,3,4,5,6-Pentafluoro-1-[2-{4-[(tetrahydrofuran-3-yl)oxyl]phenyl]ethyn-1-yl]benzene (2c)

Yield: 85%; M.p.: 106.1–107.9 °C; ¹H NMR (CDCl₃): δ 2.10–2.19 (m, 1H), 2.19–2.30 (m, 1H), 3.88–3.95 (m, 1H), 3.95–4.04 (m, 3H), 4.92–4.98 (m, 1H), 6.85 (d, *J* = 8.8 Hz, 2H), 7.50 (d, *J* = 8.8 Hz, 2H); ¹³C NMR (CDCl₃): δ 32.9, 67.1, 72.1 (q, *J* = 3.6 Hz), 72.9, 77.5, 100.5 (td, *J* = 17.6, 3.6 Hz), 101.6 (q, *J* = 2.9 Hz), 113.8, 115.4, 133.5, 136.1–139.1 (dm, *J* = 250.8 Hz), 139.5–142.8 (dm, *J* = 256.8 Hz), 145.5–148.4 (dm, *J* = 252.3 Hz), 158.4; ¹⁹F NMR (CDCl₃): δ –137.01 (dd, *J* = 21.8, 6.8 Hz, 2F), 154.02 (t, *J* = 20.3 Hz, 1F), –162.59 (ddd, *J* = 21.8, 20.3, 6.8 Hz, 2F); IR (KBr): ν 2991, 2959, 2864, 2229, 1604, 125, 1496, 1252, 1176, 1075, 987, 837 cm^{–1}; HRMS: (FAB+) *m/z* [M]⁺ calcd for C₁₈H₁₁F₅O₂: 354.0679; found: 354.0681.

1.2.1. Synthetic procedure for 2,3,5,6-tetrafluoro-4-[2-{4-[(tetrahydrofuran-3-yl)oxy]phenyl}ethyn-1-yl]benzonitrile (3c) via a nucleophilic aromatic substitution reaction

In a two-necked round-bottomed flask, equipped with a Teflon®-coated stirrer bar, was placed 4-[(tetrahydrofuran-3-yl)oxy]phenylaethylene (0.38 g, 2.0 mmol), and THF (20 mL). To the solution was added slowly a hexane solution of *n*-BuLi (1.6 mol L⁻¹; 1.4 mL, 2.2 mmol) at 0 °C, and stirred at the temperature for 0.5 h. To the resultant solution was added pentafluorobenzonitrile (3.4 g, 2.2 mL, 34.8 mmol) and the whole was stirred room temperature for 18 h. After 18 h, the resultant solution was poured into saturated aqueous NH₄Cl solution (20 mL) and the crude product was extracted with EtOAc (30 mL, three times) and organic layer combined was washed with brine (once). The collected organic layer was dried over anhydrous Na₂SO₄, which was separated by filtration. The filtrate was evaporated in vacuo and subjected to silica-gel column chromatography (eluent: hexane/EtOAc = 5/1), followed by recrystallization from CH₂Cl₂/MeOH (v/v = 1/1), to obtain the title compound in 68% (0.49 g, 1.36 mmol) as a white crystal.

2,3,5,6-Tetrafluoro-4-[2-{4-[(tetrahydrofuran-3-yl)oxy]phenyl}ethyn-1-yl]benzonitrile (3c)

Yield: 68%; M.p.: 157.4–158.1 °C; ¹H NMR (CDCl₃): δ 2.11–2.20 (m, 1H), 2.20–2.31 (m, 1H), 3.92 (td, *J* = 8.4, 4.4 Hz, 1H), 3.96–4.05 (m, 3H), 4.97 (tq, *J* = 4.4, 4.0 Hz, 1H), 6.89 (d, *J* = 8.8 Hz, 2H), 7.54 (d, *J* = 8.8 Hz, 2H); ¹³C NMR (CDCl₃): δ 32.9, 67.2, 72.9, 73.1 (q, *J* = 3.7 Hz), 77.6, 92.9 (t, *J* = 17.6 Hz), 107.3 (t, *J* = 3.7 Hz), 107.5 (t, *J* = 3.6 Hz), 111.6 (q, *J* = 17.6 Hz), 112.9, 115.6, 134.1, 146.3 (ddt, *J* = 254.5, 12.5, 4.0 Hz), 147.0 (ddt, *J* = 260.4, 15.4, 3.7 Hz), 159.2; ¹⁹F NMR (CDCl₃): δ –133.60 (ddd, *J* = 24.4, 15.0, 6.8 Hz, 2F), –134.54 (ddd, *J* = 24.4, 16.6, 6.8 Hz); IR (KBr): ν 3065, 2975, 2874, 2245, 2216, 1646, 1601, 1490, 1331, 1249, 1075, 984 cm^{–1}; HRMS: (FAB+) *m/z* [M]⁺ calcd for C₁₉H₁₁F₄NO₂: 361.0726; found: 361.0734.

2. NMR Spectra

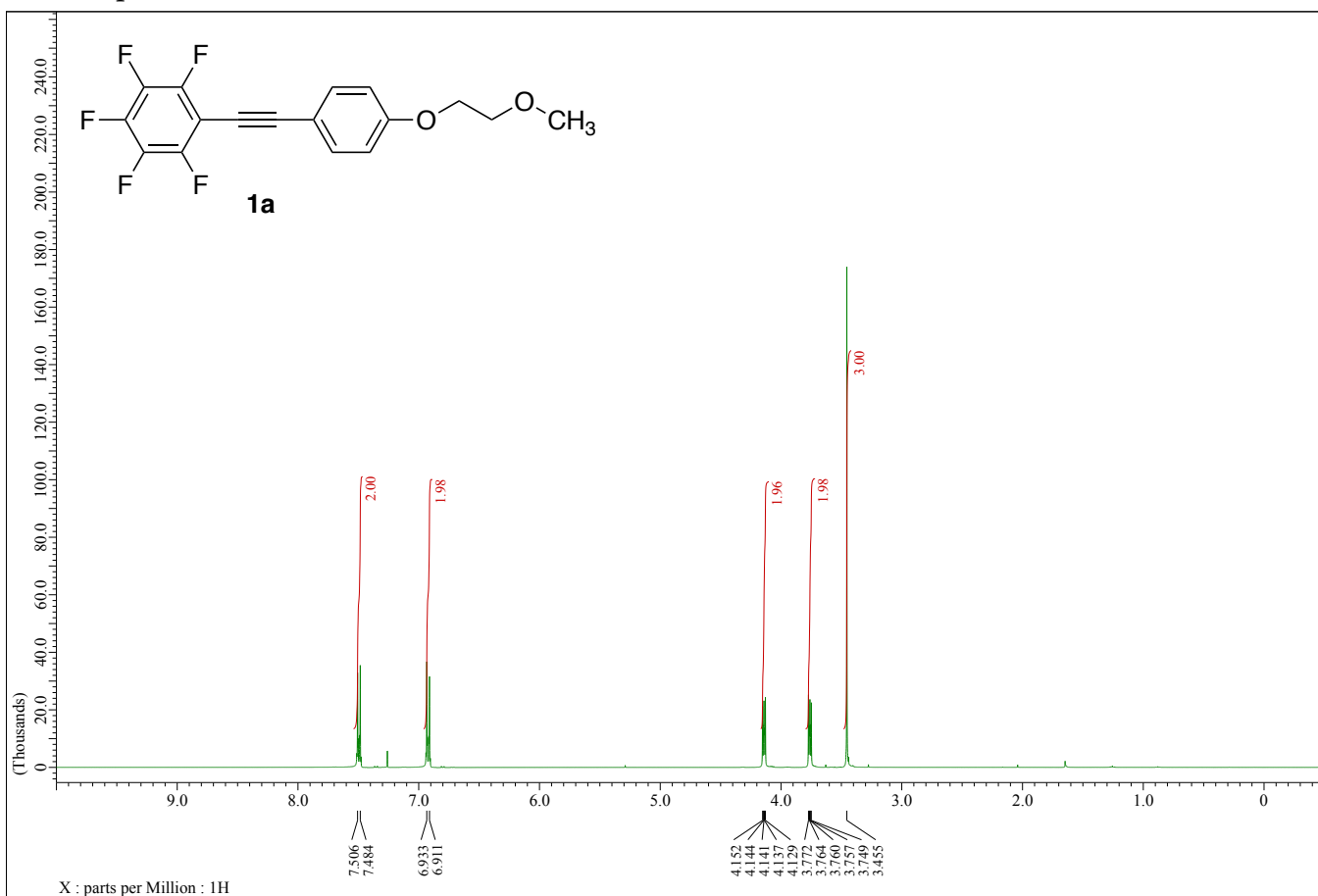


Figure S1. ¹H NMR spectrum of **1a** (400 MHz, CDCl₃)

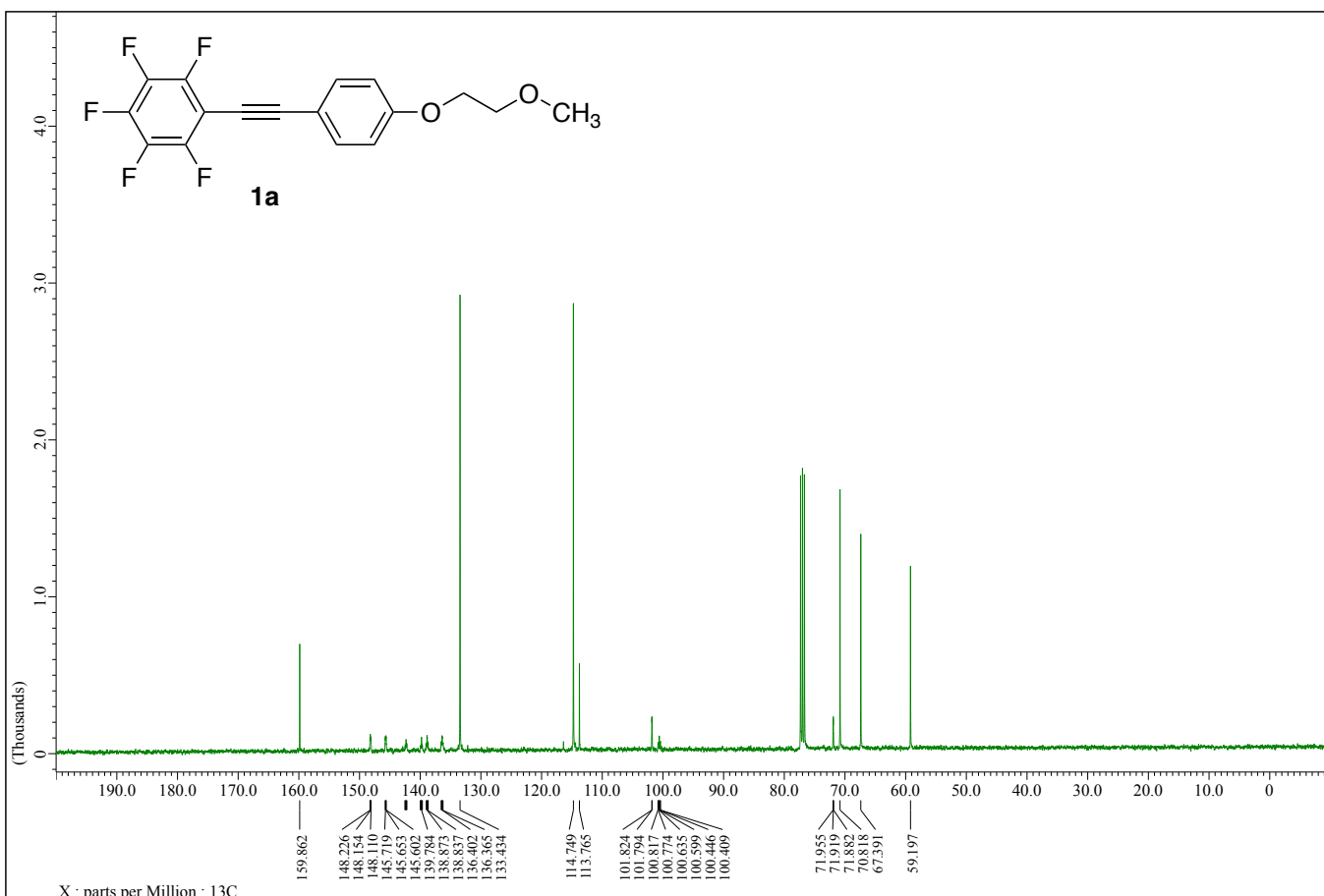
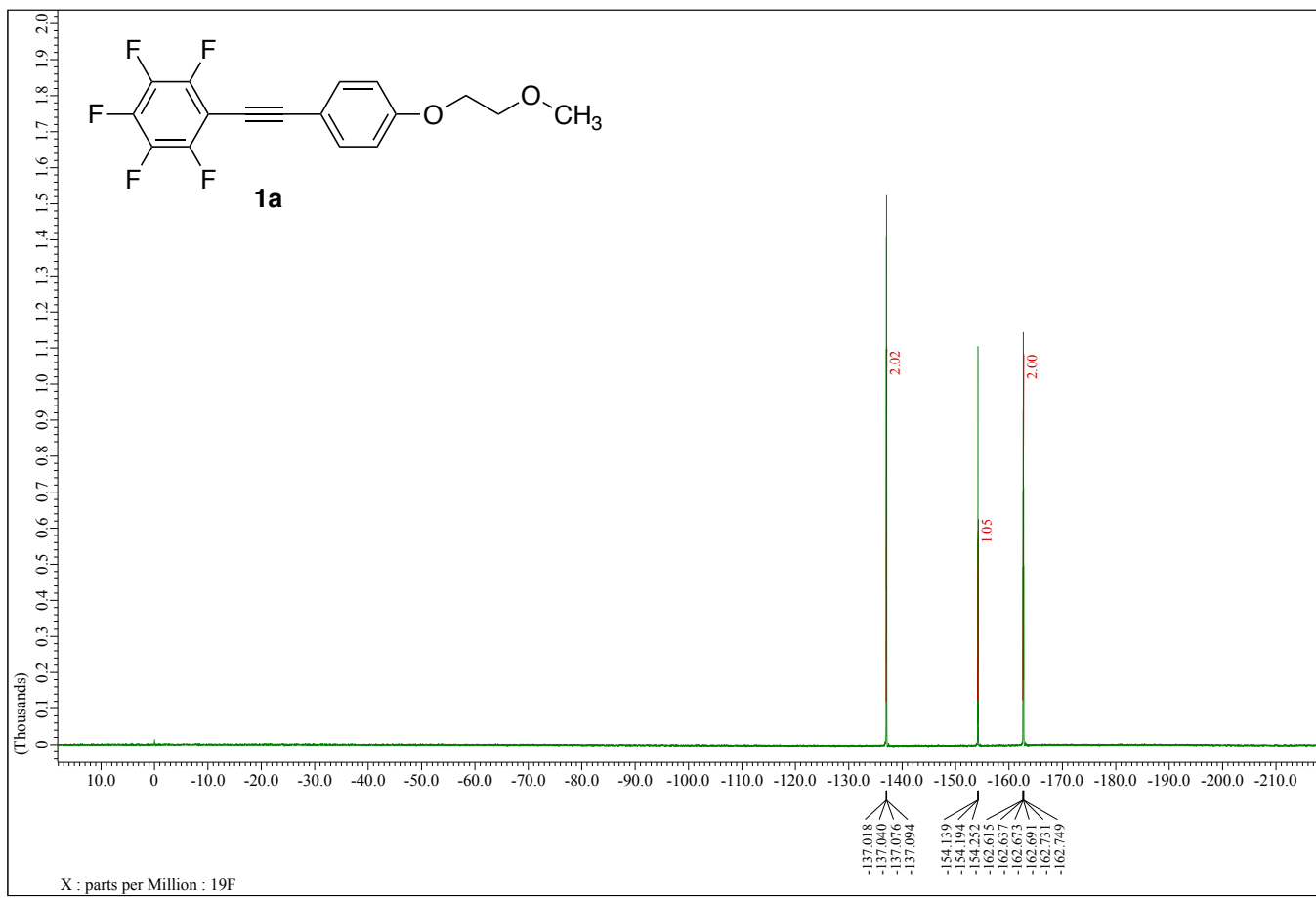


Figure S2. ¹³C NMR spectrum of **1a** (100 MHz, CDCl₃)



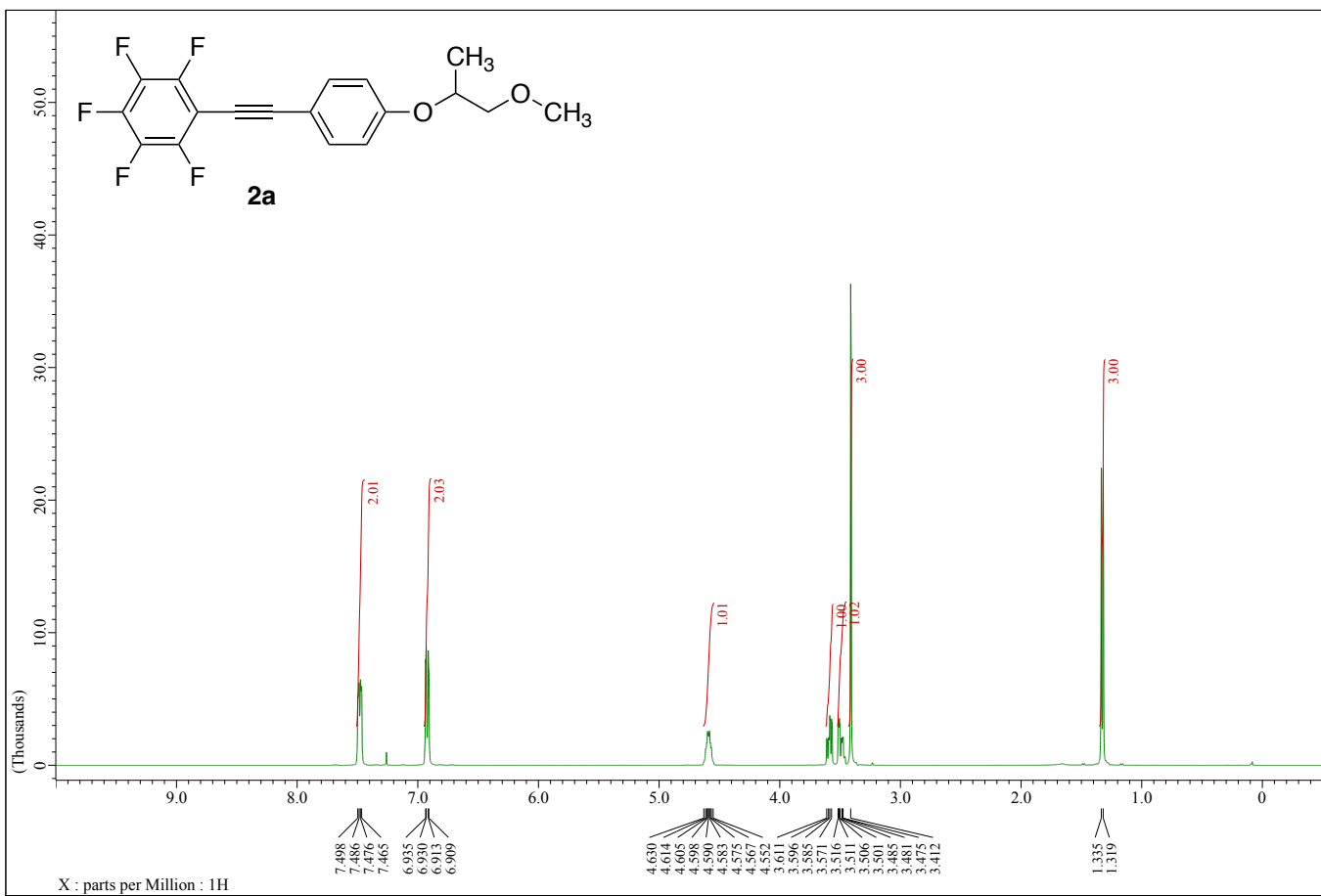


Figure S4. ^1H NMR spectrum of **2a** (400 MHz, CDCl_3)

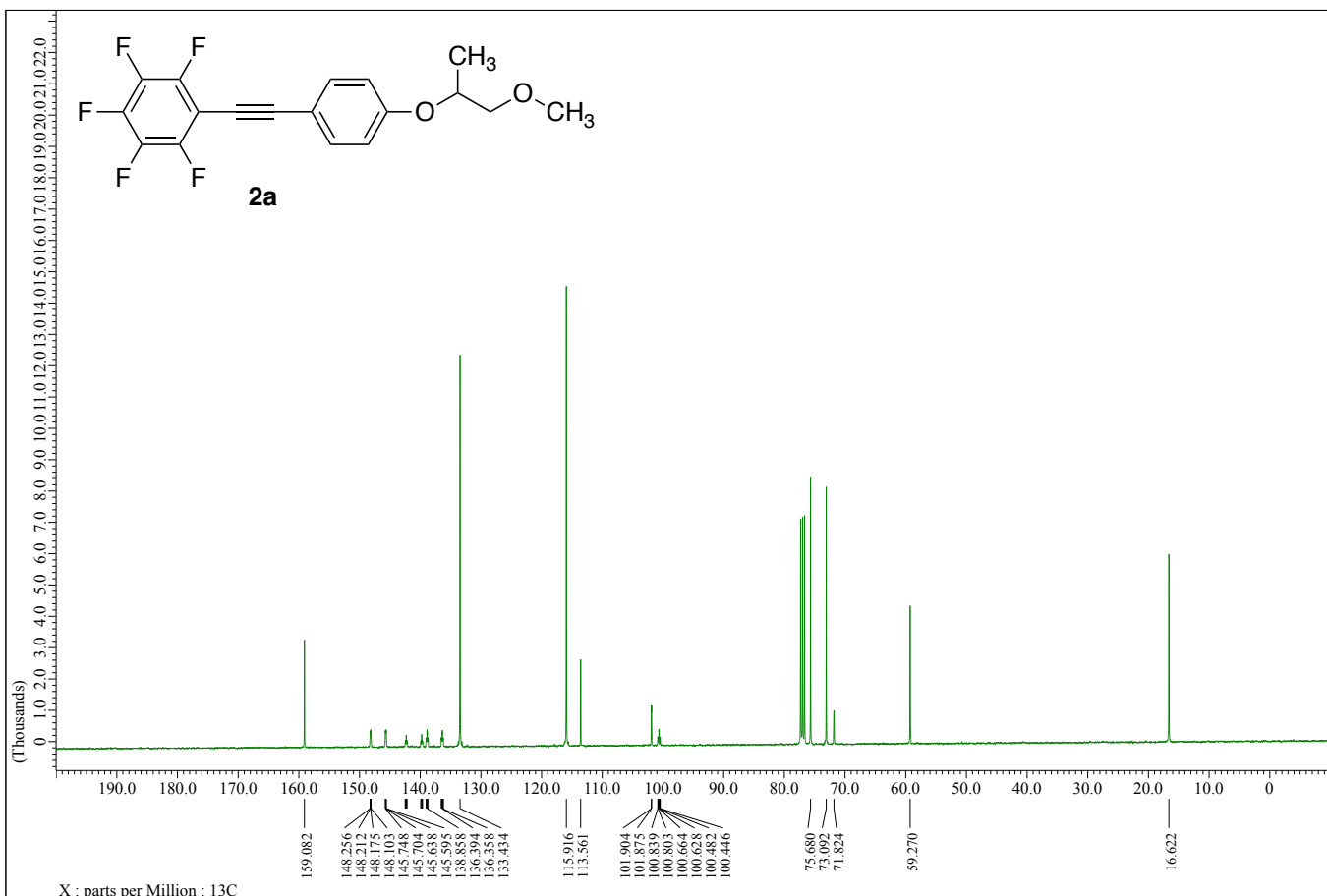
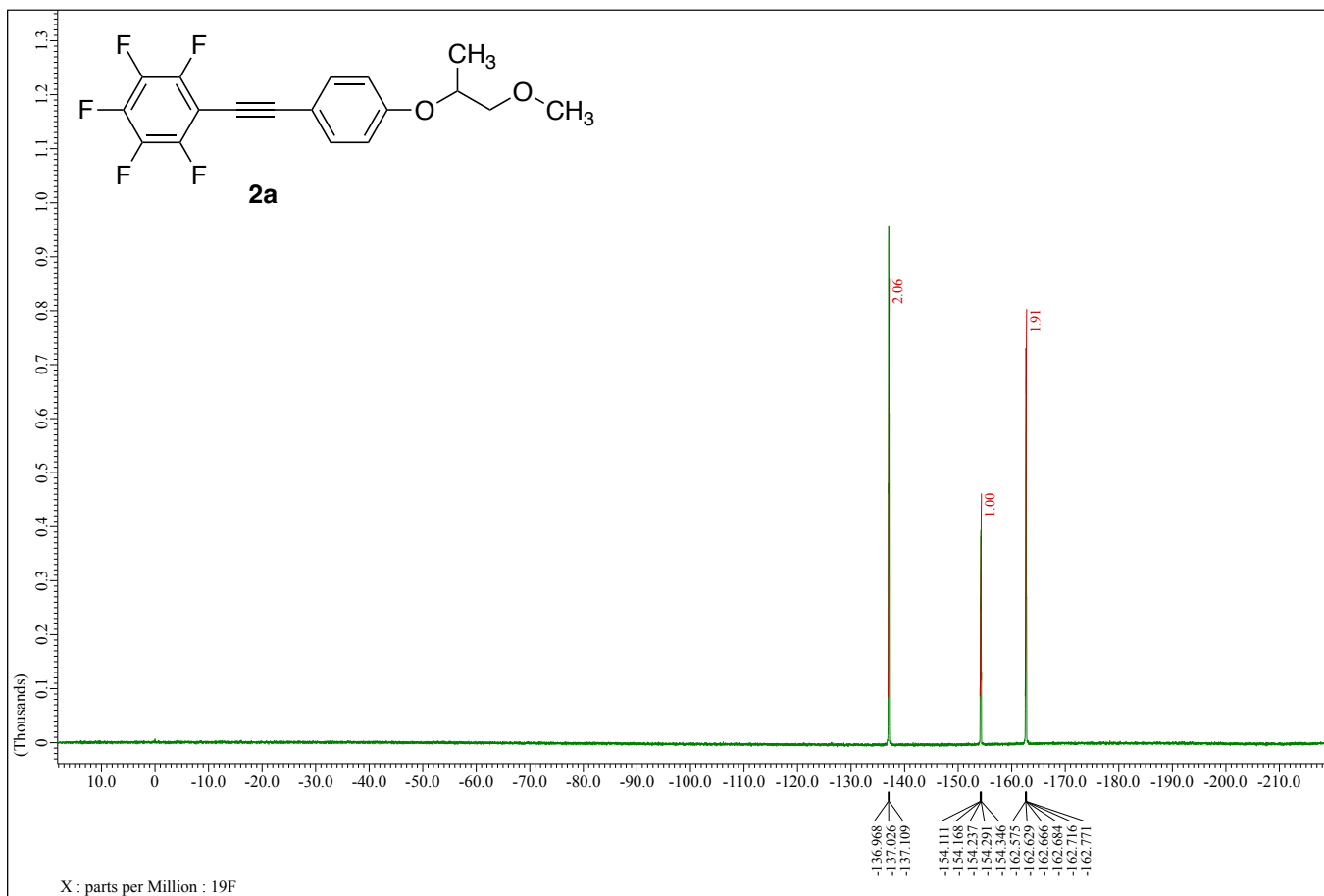


Figure S5. ^{13}C NMR spectrum of **2a** (100 MHz, CDCl_3)



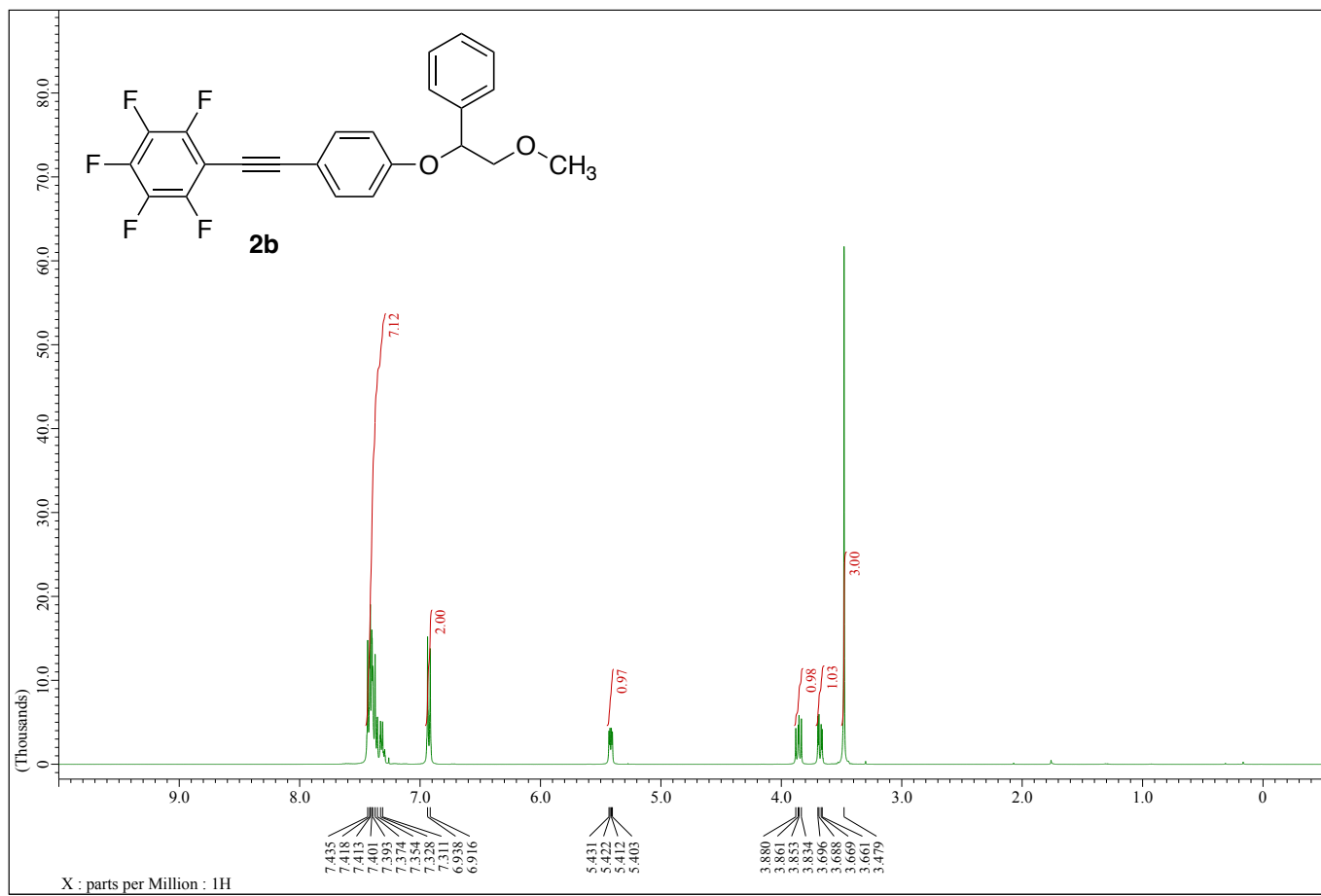


Figure S7. ^1H NMR spectrum of **2b** (400 MHz, CDCl_3)

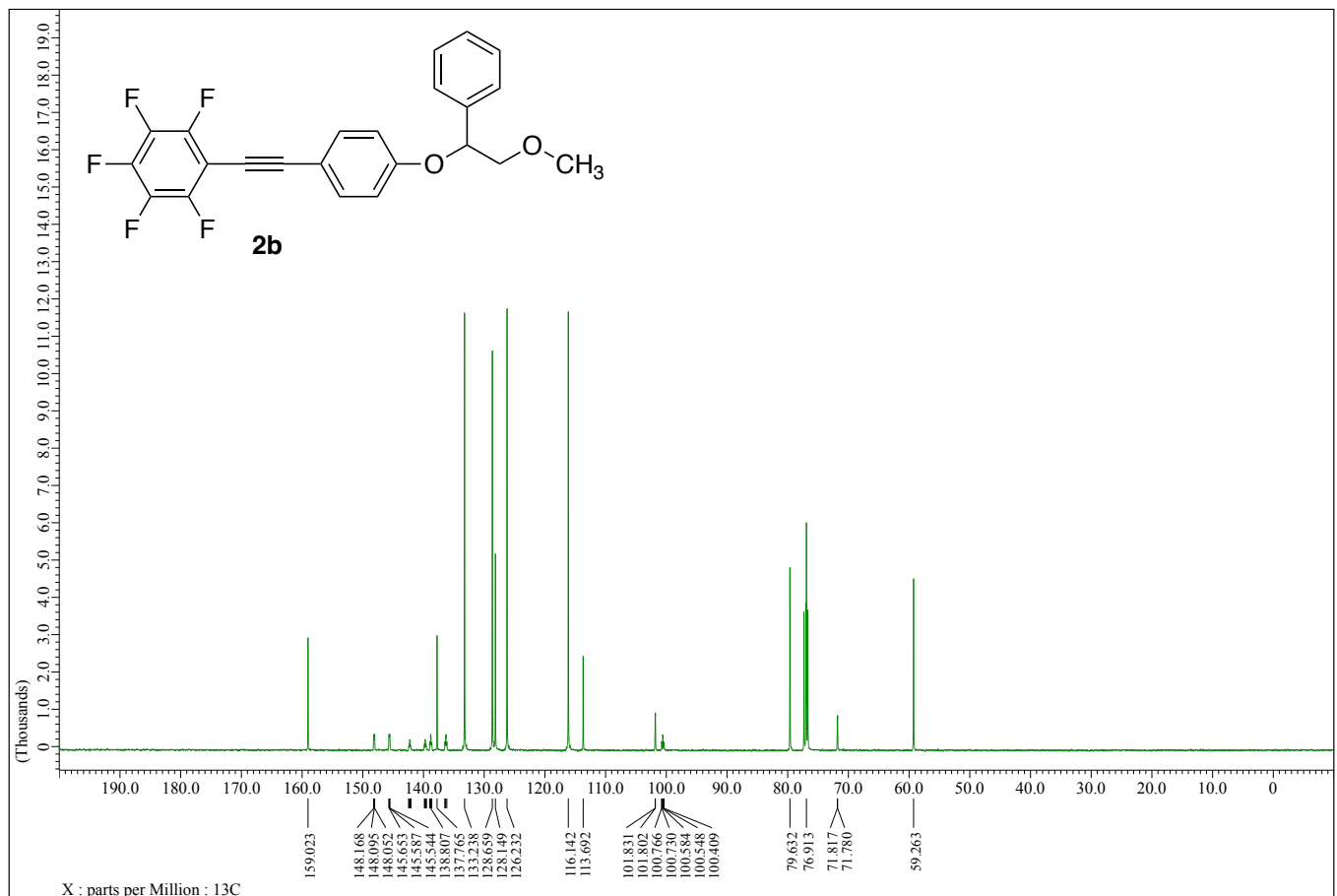


Figure S8. ^{13}C NMR spectrum of **2b** (100 MHz, CDCl_3)

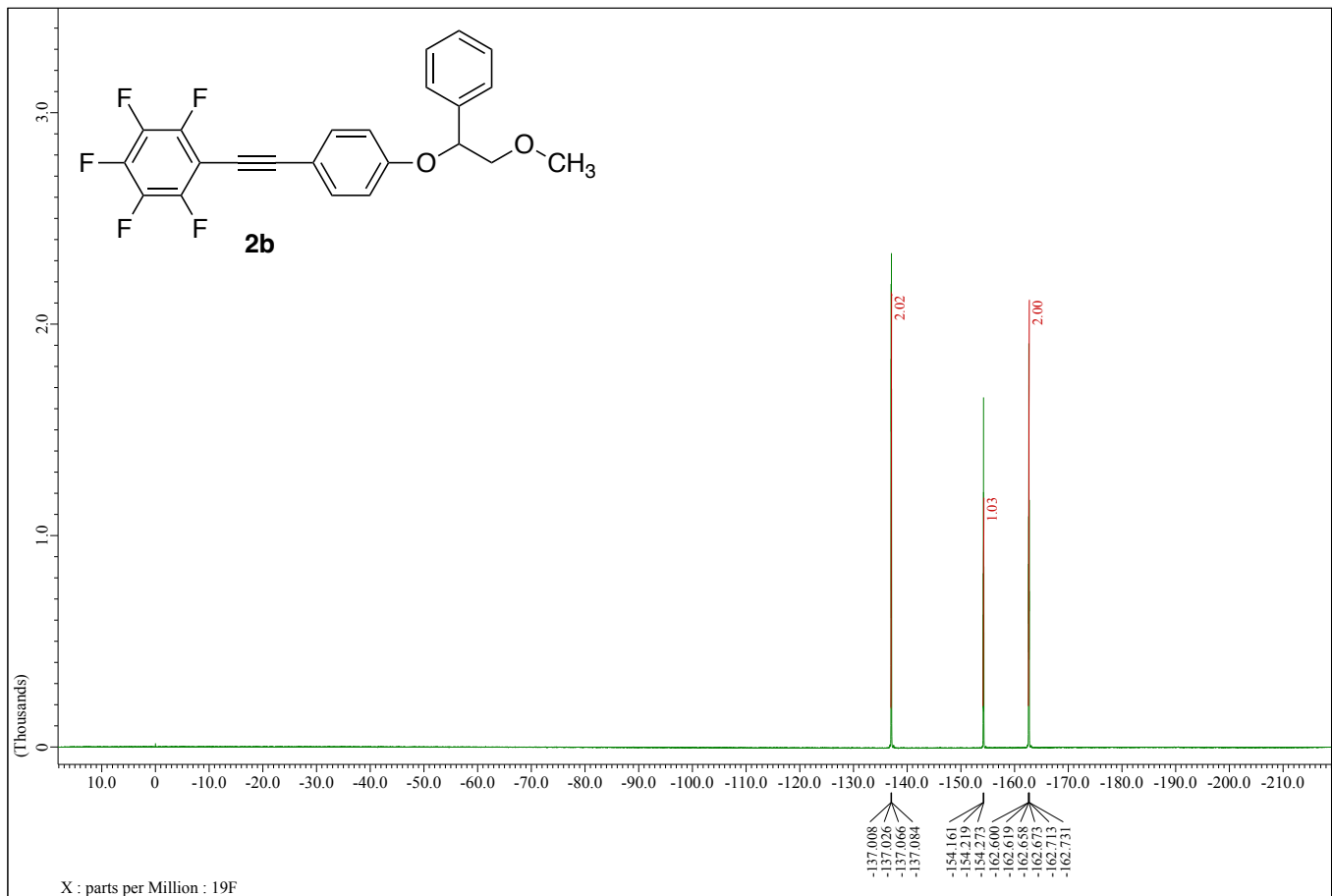


Figure S9. ^{19}F NMR spectrum of **2b** (376 MHz, CDCl_3 , CFCl_3)

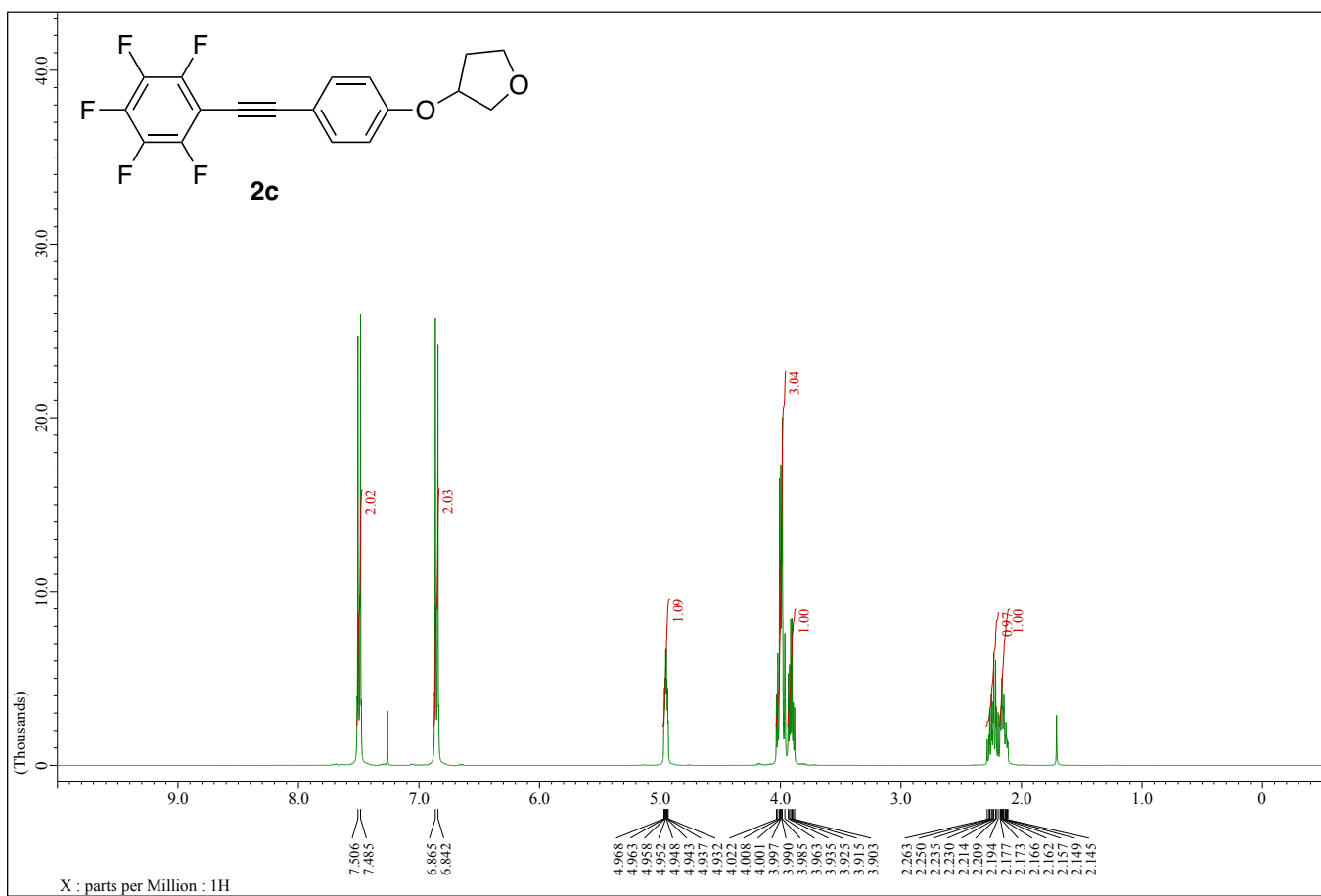


Figure S10. ^1H NMR spectrum of **2c** (400 MHz, CDCl_3)

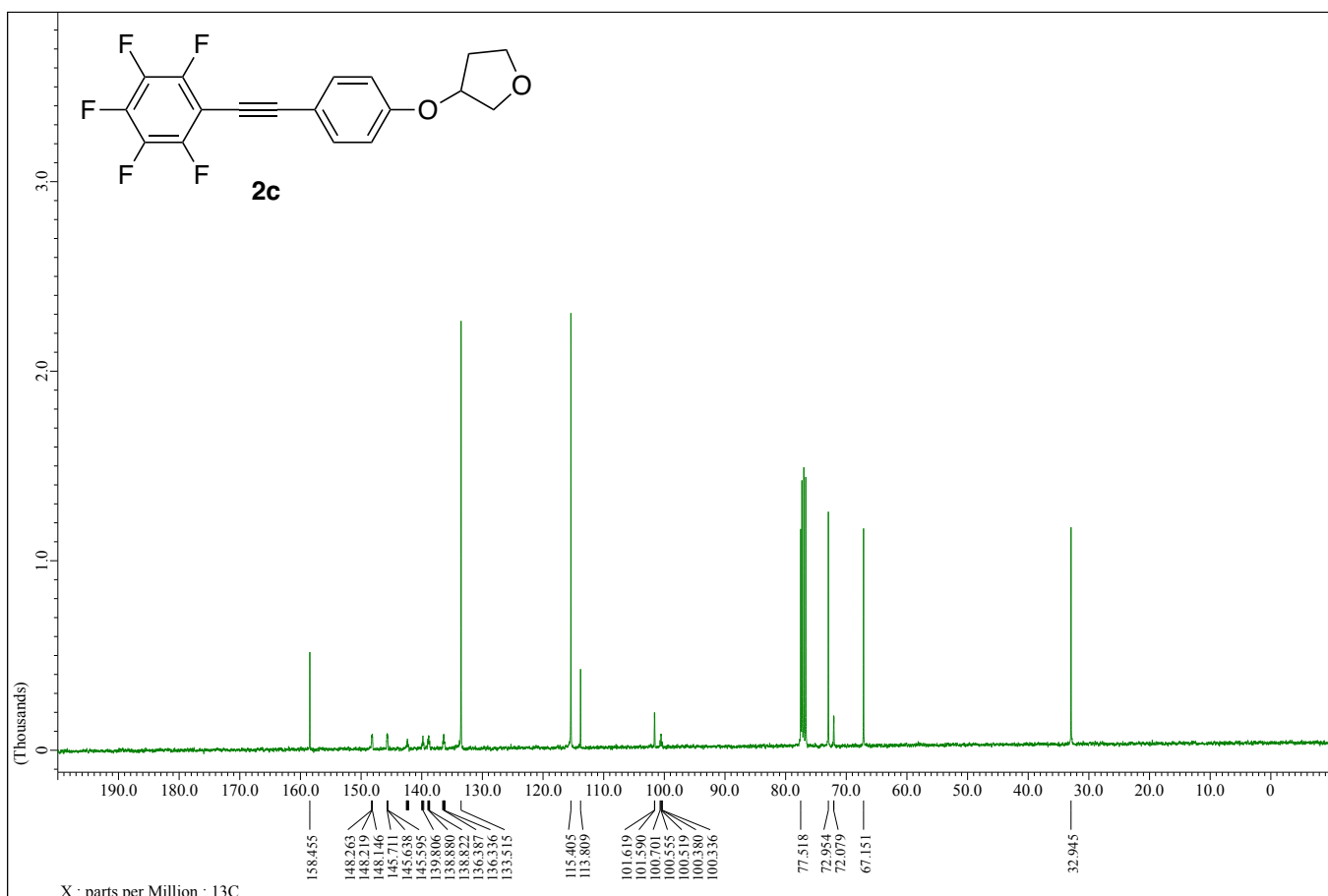


Figure S11. ^{13}C NMR spectrum of **2c** (100 MHz, CDCl_3)

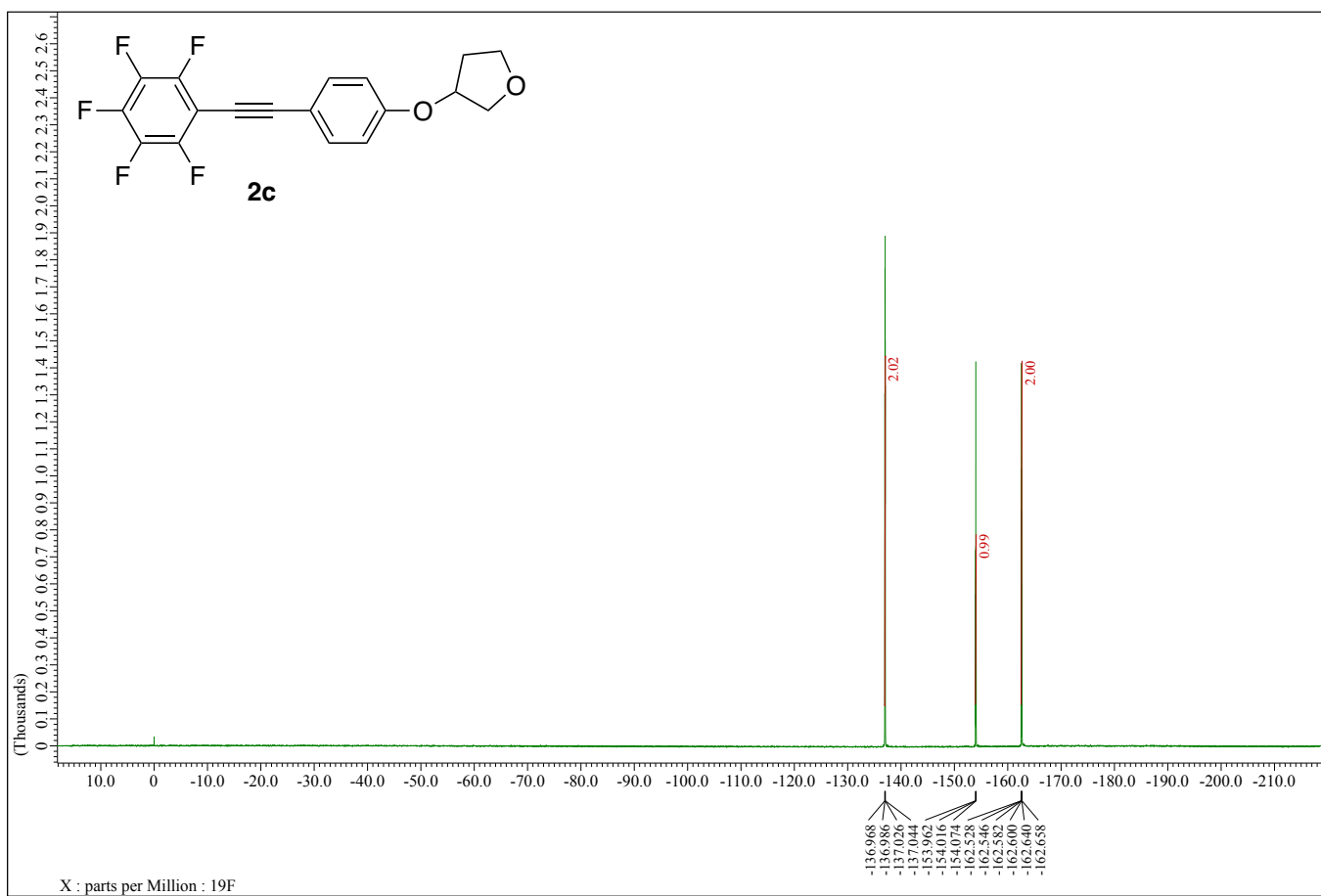


Figure S12. ¹⁹F NMR spectrum of **2c** (376 MHz, CDCl₃, CFCl₃)

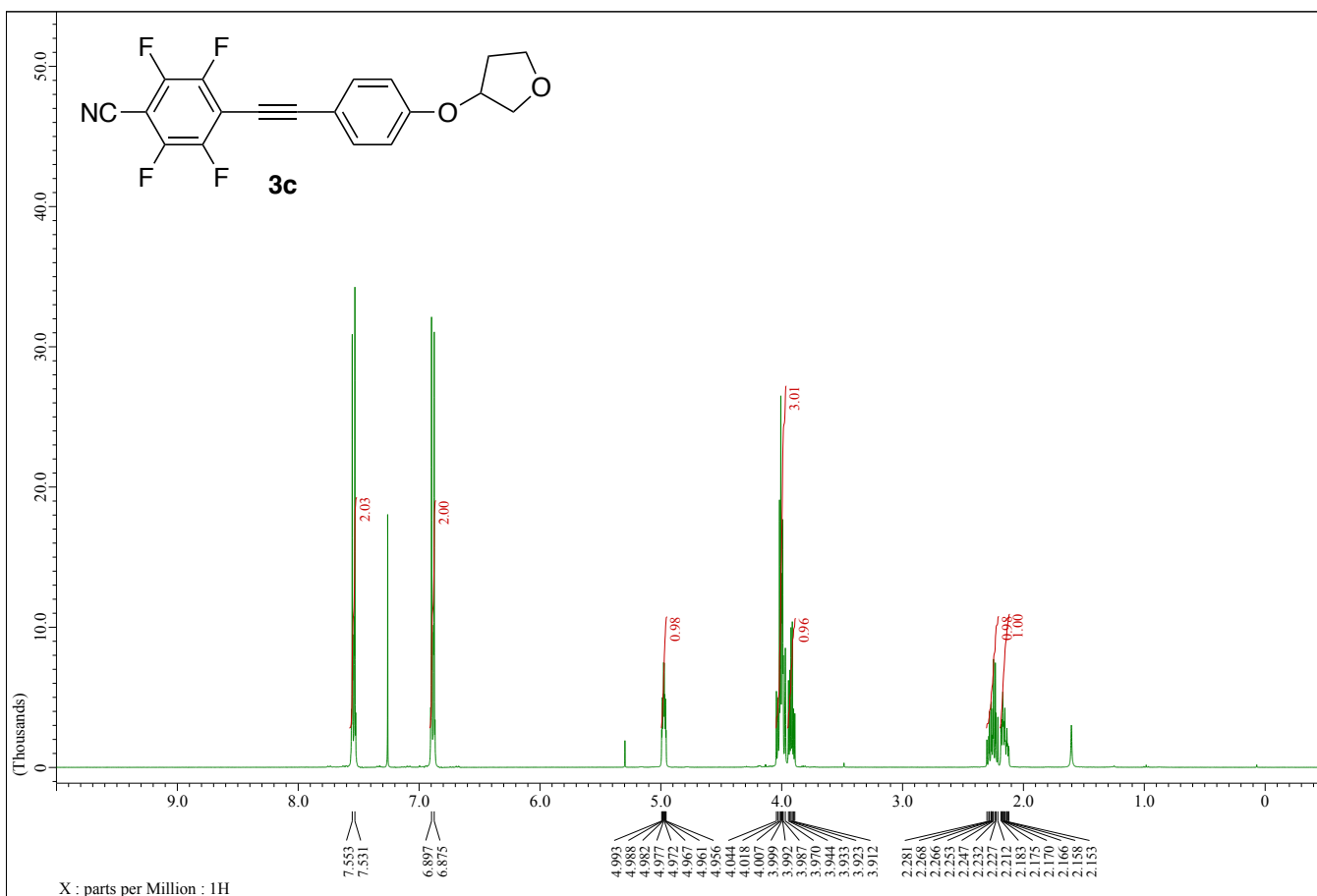


Figure S13. ^1H NMR spectrum of **3c** (400 MHz, CDCl_3)

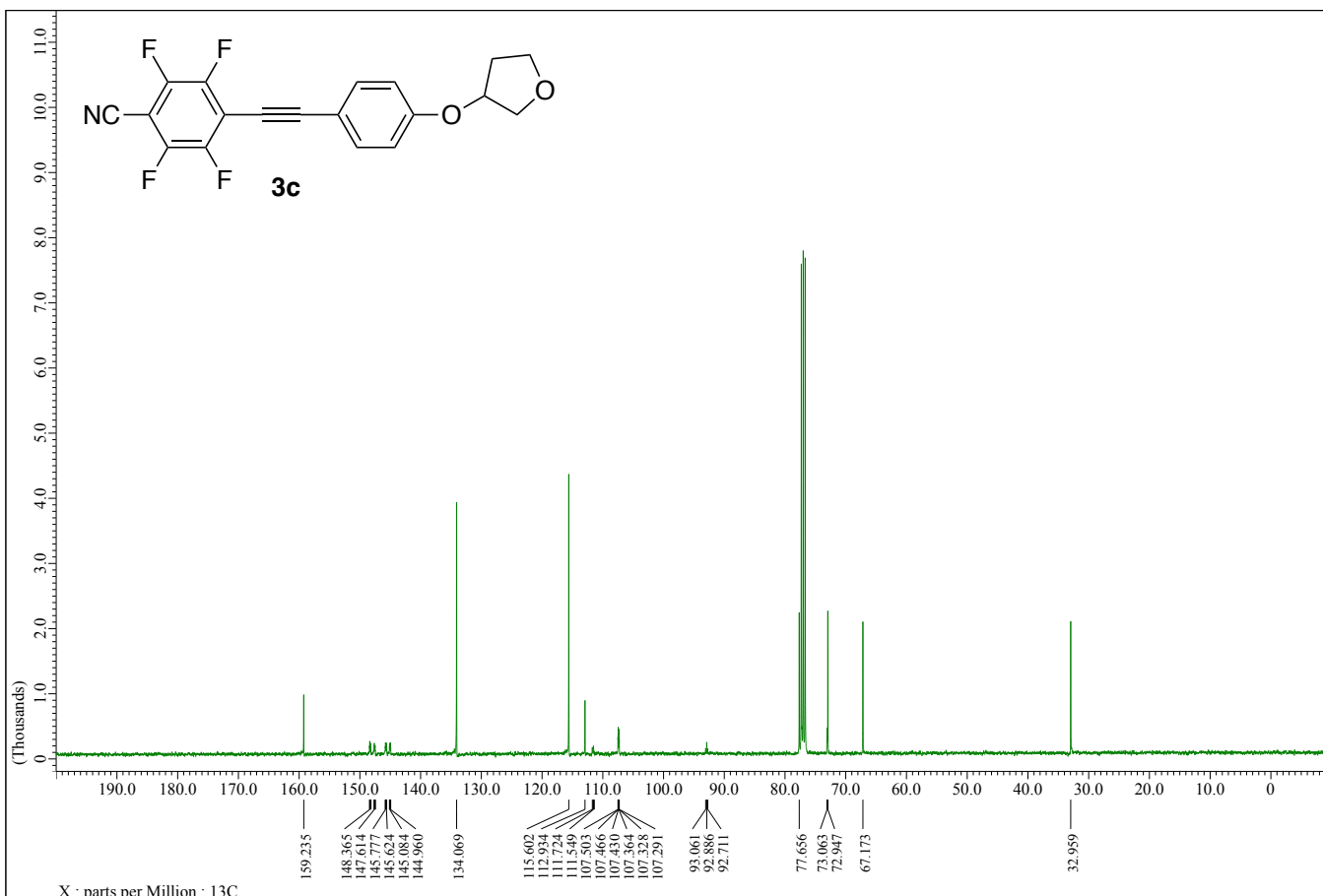


Figure S14. ^{13}C NMR spectrum of **3c** (100 MHz, CDCl_3)

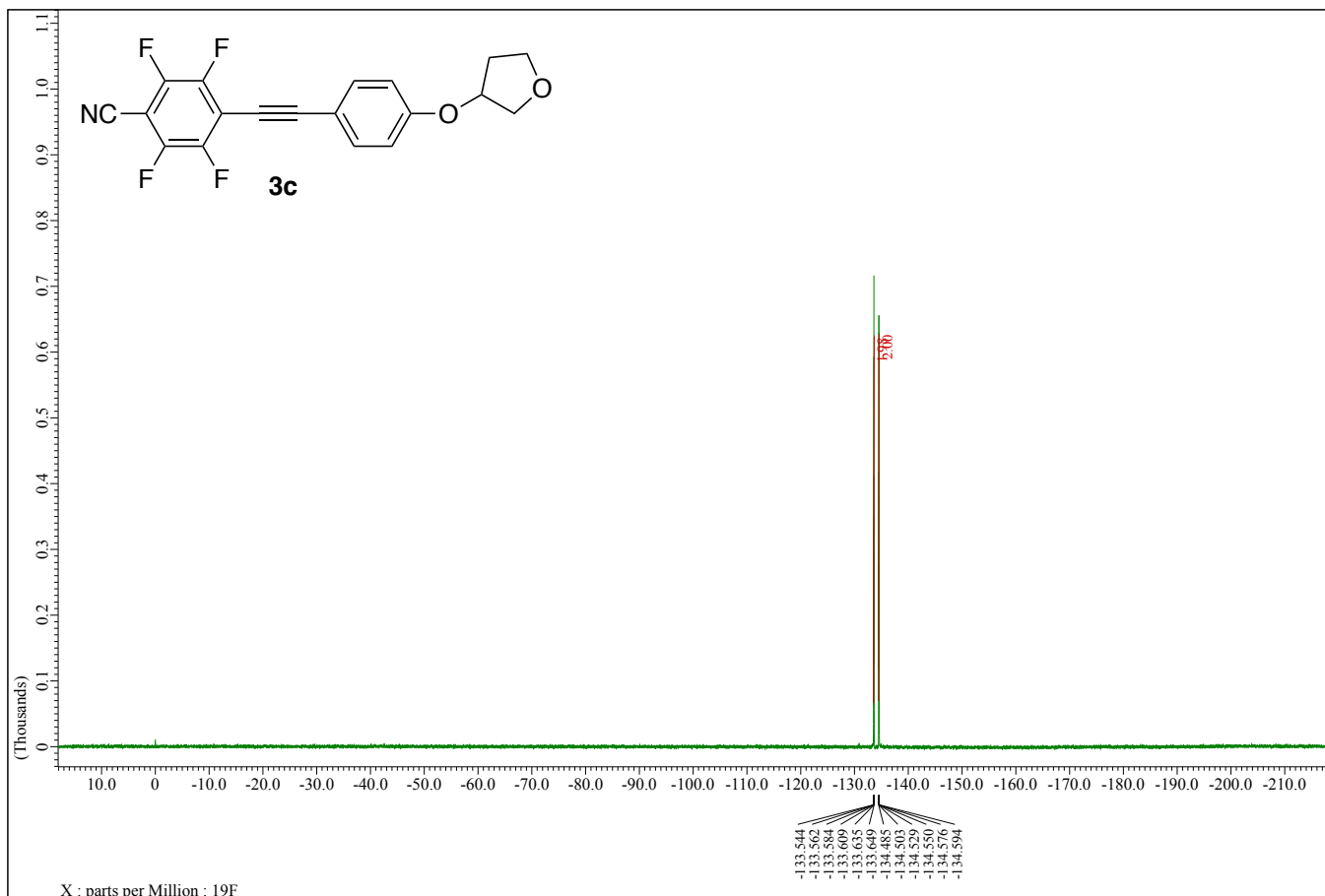


Figure S15. ¹⁹F NMR spectrum of **3c** (376 MHz, CDCl₃, CFCl₃)

3. X-ray Crystallographic Analysis

Single crystal X-ray diffractions were recorded on an XtaLab AFC11 diffractometer (Rigaku). The reflection data were integrated, scaled, and averaged using CrysAlisPro (ver. 1.171.39.43a, Rigaku). Empirical absorption corrections were applied using the SCALE 3 ABSPACK scaling algorithm (CrysAlisPro). The structure were identified by a direct method (SHELXT-2018/2) and refined using a full matrix least square method (SHELXL-2014/7) visualized by Olex2. The crystallographic data were deposited into the Cambridge Crystallographic Data Centre (CCDC) database. These data can be obtained free of charge from the CCDC via www.ccdc.cam.ac.uk/data_request/cif.

Table S1. Crystallographic data of **1a**, **2a**, **2b**, and **3c**

	1a	2a	2b	3c
CCDC #	2118480	2118481	2118482	2118483
Empirical Formula	C ₁₇ H ₁₁ F ₅ O ₂	C ₁₈ H ₁₃ F ₅ O ₂	C ₂₃ H ₁₅ F ₅ O ₂	C ₁₉ H ₁₁ F ₄ NO ₂
Formula weight	342.26	356.28	418.35	361.29
Temperature [K]	299	293	299	298
Crystal Habit	Colorless / Block	Colorless / Block	Colorless / Block	Colorless / Block
Crystal Size [mm]	0.94 x 0.67 x 0.26	0.55 x 0.48 x 0.43	0.55 x 0.48 x 0.43	0.52 x 0.34 x 0.20
Crystal System	Monoclinic	Triclinic	Triclinic	Monoclinic
Space Group	P1 2 ₁ /c 1	P -1	P -1	P1 2 ₁ /n 1
<i>a</i> [Å]	8.9965(3)	7.5715(6)	8.9679(5)	6.1206(3)
<i>b</i> [Å]	7.9831(3)	10.6727(6)	9.2898(4)	22.0913(10)
<i>c</i> [Å]	21.5960(9)	11.9855(7)	11.8018(5)	11.8054(6)
α [°]	90	65.696(6)	88.321(4)	90
β [°]	94.474(4)	71.888(6)	83.008(4)	97.582(5)
γ [°]	90	76.943(6)	84.421(4)	90
<i>V</i> [Å ³]	1546.30(10)	833.57(11)	971.12(8)	1582.28(13)
<i>Z</i>	4	2	2	4
<i>R</i> [$F^2 > 2\sigma(F^2)$] ^[a]	0.0510	0.1432	0.0447	0.0485
<i>wR</i> ₂ (F^2) ^[b]	0.1624	0.5001	0.1381	0.1503

[a] $R = \sum ||F_o|| - |F_c|| / \sum |F_o||$. [b] $wR = \{[\sum w(|F_o| - |F_c|)] / \sum w|F_o|\}^{1/2}$.

4. DFT calculation

All computations were performed using the Gaussian 16 software package (Revision B.01). Geometry optimizations were carried out using the CAM-B3LYP hybrid functional and the 6-31+G(d) basis set with an implicit solvation model (conductor-like polarizable continuum model; CPCM) for CH₂Cl₂. The vertical excitation energies and dipole moments of the optimized structures were calculated using the time-dependent self-consistent field approximation at the same level of theory.

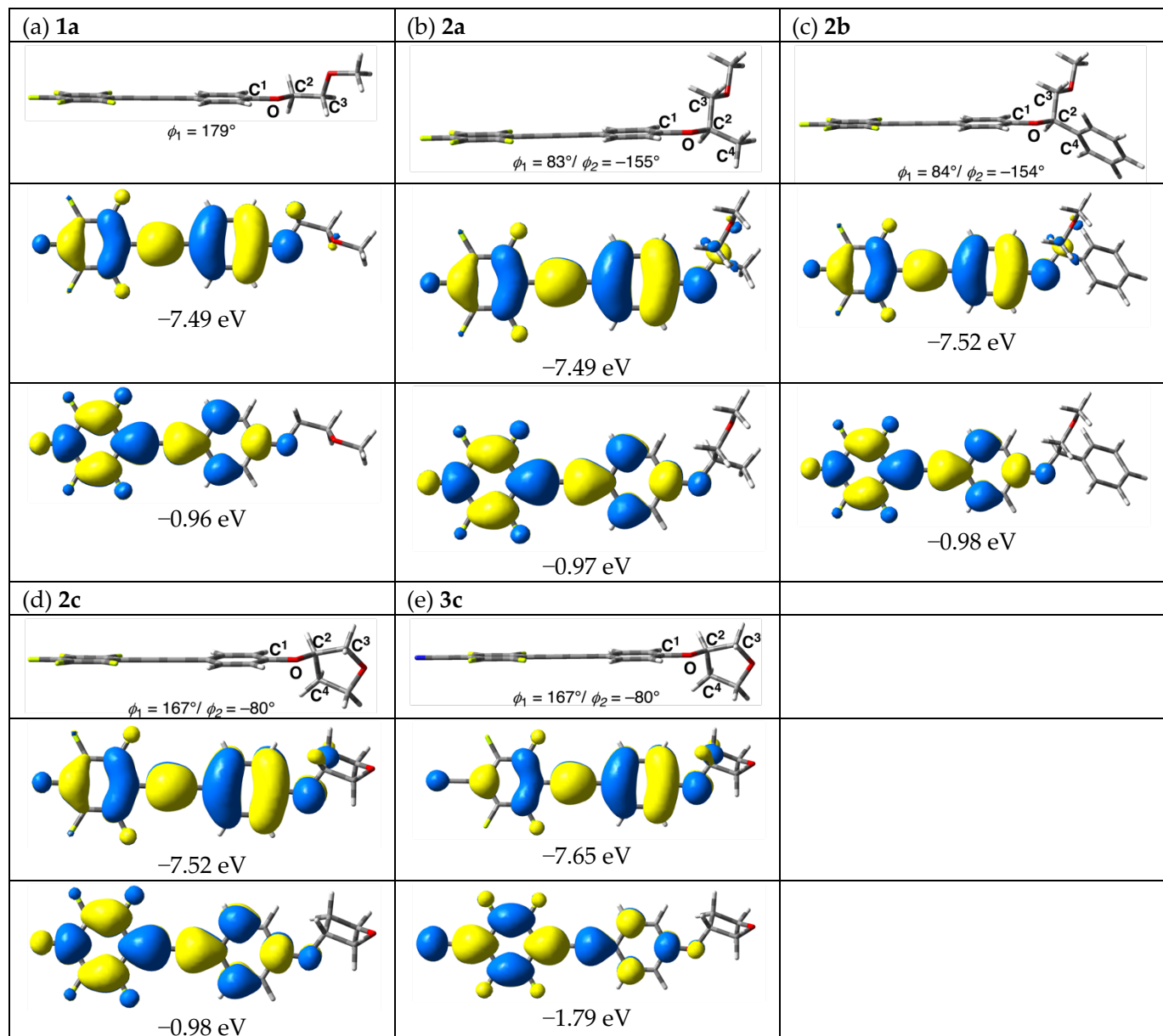


Figure S16. Optimized geometry, HOMO and LUMO distributions for **1a**, **2a–c**, and **3c** at S₀ state.

Table S2. Energy (hartree) and dipole moment (debye) of **1a**, **2a–c**, and **3c** at S_0 state.

	E(RCAM-B3LYP) [hartree]	Dipole moment (debye)
1a	-1303.82476447	X= -6.1818/ Y= -1.8659/ Z= -1.4624/ Tot= 6.6208
2a	-1343.12614784	X= 4.8136/ Y= 0.7952/ Z= 1.0909/ Tot= 4.9994
2b	-1534.79588633	X= -4.5082/ Y= 1.2126/ Z= -1.3888/ Tot= 4.8706
2c	-1341.92350211	X= -2.7877/ Y= 1.3028/ Z= -0.0075/ Tot= 3.0780
3c	-1334.90603360	X= 7.2520/ Y= -1.0002/ Z= -0.0879/ Tot= 7.3212

Table S3. Theoretical vertical transition behavior calculated by TD-DFT calculation.

	Transition	Transition Energy (eV)	Theoretical Absorption (nm)	Oscillator strength <i>f</i>
1a	HOMO → LUMO	4.1422	299.32	1.3106
2a	HOMO → LUMO	4.1375	299.66	1.3205
2b	HOMO → LUMO	4.1424	299.30	1.4127
2c	HOMO → LUMO	4.1484	298.87	1.3183
3c	HOMO → LUMO	3.7157	333.68	1.4966

Table S4. Cartesian coordinate for **1a** at the optimized geometry in S_0 state.

No.	Atom	Type	Coordinates (Angstroms)			18	1	0	-3.721218	-2.028557	-0.164329
			No.	x	y	z					
1	8	0	-5.203326	0.256400	-0.357394	20	6	0	0.368940	0.060387	-0.112360
2	9	0	3.044482	-2.345669	0.050790	21	6	0	-1.793459	-1.104108	-0.136206
3	9	0	5.736243	-2.384312	0.166235	22	1	0	-1.273990	-2.053927	-0.061096
4	9	0	7.137053	-0.052237	0.176137	23	6	0	1.577332	0.042016	-0.061410
5	9	0	3.129055	2.379295	-0.045803	24	6	0	3.749555	1.195638	0.005877
6	9	0	5.820602	2.326158	0.069924	25	6	0	-6.010546	-0.917129	-0.313918
7	6	0	-3.856030	0.130249	-0.291407	26	1	0	-5.823210	-1.465389	0.616275
8	8	0	-7.825354	0.138468	0.815661	27	1	0	-5.773032	-1.564169	-1.166381
9	6	0	-3.128852	1.326994	-0.328413	28	6	0	5.131536	1.181100	0.064968
10	1	0	-3.669092	2.264932	-0.403283	29	6	0	-7.457291	-0.501549	-0.387149
11	6	0	-1.748967	1.304921	-0.270004	30	1	0	-7.611230	0.172547	-1.242386
12	1	0	-1.192389	2.235994	-0.299119	31	1	0	-8.072628	-1.399997	-0.544460
13	6	0	2.995963	0.018339	-0.001015	32	6	0	-9.169302	0.577830	0.808485
14	6	0	-1.056918	0.084556	-0.172633	33	1	0	-9.341440	1.308062	0.006037
15	6	0	3.707054	-1.183833	0.054577	34	1	0	-9.359925	1.050836	1.773081
16	6	0	5.088648	-1.216445	0.114044	35	1	0	-9.860064	-0.266362	0.675697
17	6	0	-3.182585	-1.089816	-0.194678						

Table S5. Cartesian coordinate for **2a** at the optimized geometry in S_0 state.

No.	Atom	Type	Coordinates (Angstroms)			19	6	0	-1.761056	-0.215441	-0.079901
			No.	x	y						
1	8	0	4.947143	-1.279564	-0.294053	21	1	0	0.746058	-2.690226	0.284577
2	9	0	-2.960945	2.269344	-0.585529	22	6	0	5.936142	-0.280603	-0.583798
3	9	0	-7.268236	0.555491	0.146469	23	1	0	5.550676	0.407130	-1.343187
4	9	0	-3.551640	-2.282563	0.542631	24	6	0	-5.948872	0.370578	0.090938
5	6	0	-3.166494	-0.019055	-0.024870	25	6	0	-5.410386	-0.880781	0.348186
6	6	0	3.624913	-0.972092	-0.263955	26	6	0	-5.110775	1.429041	-0.224305
7	9	0	-6.217040	-1.902021	0.652102	27	6	0	6.241554	0.492340	0.695380
8	6	0	0.848470	-0.582617	-0.172666	28	1	0	5.313068	0.862025	1.153201
9	9	0	-5.628328	2.635837	-0.472901	29	1	0	6.733473	-0.175143	1.419109
10	6	0	3.089456	0.297181	-0.498328	30	6	0	7.145060	-1.011773	-1.131703
11	1	0	3.723189	1.148742	-0.711042	31	1	0	7.506105	-1.749104	-0.407391
12	6	0	-4.040548	-1.063837	0.288843	32	1	0	7.948094	-0.298489	-1.333544
13	6	0	1.712479	0.481331	-0.453646	33	1	0	6.892500	-1.527986	-2.061898
14	1	0	1.302837	1.469486	-0.636266	34	8	0	7.085285	1.573876	0.365454
15	6	0	-3.743194	1.228611	-0.279229	35	6	0	7.447071	2.349168	1.492081
16	6	0	2.768381	-2.043587	0.019732	36	1	0	7.995328	1.743788	2.226471
17	1	0	3.200754	-3.022291	0.199670	37	1	0	6.559471	2.779136	1.975737
18	6	0	-0.563826	-0.382303	-0.123986	38	1	0	8.090448	3.155375	1.136221

Table S6. Cartesian coordinate for **2b** at the optimized geometry in S_0 state.

No.	Atom	Type	Coordinates (Angstroms)			23	1	0	-4.247963	0.910628	0.854644
			No.	x	y	z					
1	8	0	-3.714414	-0.705217	-0.339212	25	6	0	6.668937	-1.058433	-0.293921
2	9	0	4.379697	2.125493	0.896651	26	6	0	6.487220	1.171653	0.570261
3	9	0	8.600786	0.185344	0.231593	27	6	0	-4.814847	1.252986	-1.194426
4	9	0	4.737587	-2.268937	-0.806667	28	1	0	-3.833437	1.599363	-1.548133
5	6	0	4.468392	-0.077461	0.040802	29	1	0	-5.294629	0.699128	-2.014211
6	6	0	-2.372676	-0.501629	-0.256506	30	8	0	-5.607788	2.348471	-0.800567
7	9	0	7.423660	-2.091345	-0.680426	31	6	0	-5.851531	3.255336	-1.859341
8	6	0	0.423123	-0.329585	-0.138967	32	1	0	-6.390806	2.764562	-2.680546
9	9	0	7.066742	2.289549	1.017937	33	1	0	-4.911199	3.670216	-2.246822
10	6	0	-1.763753	0.688942	0.146519	34	1	0	-6.464066	4.063405	-1.456699
11	1	0	-2.344998	1.562723	0.412870	35	6	0	-5.925411	-0.332153	0.444018
12	6	0	5.289203	-1.137654	-0.354391	36	6	0	-6.513696	0.004409	1.661753
13	6	0	-0.376996	0.765272	0.204575	37	6	0	-6.547232	-1.280192	-0.372352
14	1	0	0.090572	1.692711	0.518774	38	6	0	-7.710367	-0.589300	2.059444
15	6	0	5.108940	1.075651	0.503268	39	1	0	-6.035361	0.737960	2.305290
16	6	0	-1.581360	-1.603010	-0.605507	40	6	0	-7.737299	-1.880320	0.025333
17	1	0	-2.071536	-2.519485	-0.916720	41	1	0	-6.093877	-1.558149	-1.319471
18	6	0	1.846350	-0.240175	-0.076669	42	6	0	-8.323882	-1.533876	1.242185
19	6	0	3.052476	-0.166969	-0.023431	43	1	0	-8.158647	-0.315655	3.009931
20	6	0	-0.203421	-1.519409	-0.547854	44	1	0	-8.209117	-2.619355	-0.615478
21	1	0	0.401111	-2.378972	-0.818306	45	1	0	-9.254275	-2.001038	1.551152
22	6	0	-4.640436	0.332745	0.013314						

Table S7. Cartesian coordinate for **2c** at the optimized geometry in S_0 state.

No.	Atom	Type	Coordinates (Angstroms)			18	1	0	-3.392814	-2.660364	0.125672
			No.	x	y						
1	9	0	3.416456	-2.366132	0.123979	20	6	0	-1.704331	0.786828	-0.316167
2	9	0	5.728198	2.548625	-0.062987	21	1	0	-1.238004	1.758958	-0.438857
3	9	0	3.042434	2.339054	-0.125104	22	6	0	1.723908	-0.134475	-0.038350
4	9	0	6.101202	-2.142178	0.185298	23	6	0	-3.090383	0.686323	-0.358809
5	8	0	-5.036189	-0.781509	-0.237621	24	1	0	-3.677389	1.583978	-0.506497
6	8	0	-8.230855	0.276904	0.079540	25	6	0	-5.927004	0.303089	-0.524791
7	6	0	3.139150	-0.020828	-0.002850	26	1	0	-5.537280	0.856271	-1.382602
8	6	0	-0.903793	-0.342252	-0.113789	27	6	0	-7.305020	-0.318566	-0.822164
9	6	0	-3.696940	-0.562437	-0.202606	28	1	0	-7.655367	-0.125350	-1.837385
10	6	0	5.941115	0.205308	0.061314	29	1	0	-7.247362	-1.402008	-0.658086
11	6	0	3.963667	-1.146724	0.077095	30	6	0	-6.186471	1.196119	0.697908
12	6	0	5.342864	-1.044457	0.109148	31	1	0	-5.365023	1.160810	1.416961
13	6	0	5.153032	1.343209	-0.017479	32	1	0	-6.323469	2.233604	0.378222
14	6	0	-1.528263	-1.591350	0.048399	33	6	0	-7.496170	0.639114	1.246432
15	1	0	-0.922288	-2.477412	0.206973	34	1	0	-7.322206	-0.246917	1.873416
16	6	0	3.775355	1.222963	-0.048554	35	1	0	-8.091112	1.361769	1.806938
17	6	0	-2.904920	-1.698849	0.004828	36	9	0	7.269778	0.312729	0.091660

Table S8. Cartesian coordinate for **3c** at the optimized geometry in S_0 state.

No.	Atom	Type	Coordinates (Angstroms)			19	6	0	-0.309465	0.241216	-0.088235
	No.	x	y	z							
1	9	0	-3.188937	2.389880	0.134412	21	1	0	1.433331	-1.766291	-0.389306
2	9	0	-5.504752	-2.514775	-0.088141	22	6	0	-1.515978	0.151961	-0.052914
3	9	0	-2.835455	-2.314104	-0.157968	23	6	0	3.290764	-0.701200	-0.340375
4	9	0	-5.857703	2.180696	0.203095	24	1	0	3.874101	-1.605457	-0.458767
5	8	0	5.241460	0.760565	-0.261570	25	6	0	-7.170674	-0.281360	0.098081
6	8	0	8.430344	-0.294364	0.105363	26	7	0	-8.323075	-0.370102	0.129484
7	6	0	-2.927095	0.044443	-0.014014	27	6	0	6.129566	-0.337132	-0.509041
8	6	0	1.110656	0.346705	-0.131369	28	1	0	5.740046	-0.917117	-1.348902
9	6	0	3.902970	0.549778	-0.222195	29	6	0	7.510663	0.269268	-0.822672
10	6	0	-5.748940	-0.172218	0.059558	30	1	0	7.865042	0.036579	-1.828177
11	6	0	-3.744957	1.175945	0.078996	31	1	0	7.455558	1.358298	-0.700219
12	6	0	-5.120621	1.072651	0.114686	32	6	0	6.381187	-1.188187	0.744481
13	6	0	-4.941760	-1.306897	-0.033166	33	1	0	5.556332	-1.127787	1.457955
14	6	0	1.740213	1.598352	-0.007581	34	1	0	6.518123	-2.235969	0.460454
15	1	0	1.137818	2.491484	0.121751	35	6	0	7.689073	-0.614767	1.280286
16	6	0	-3.566548	-1.198970	-0.068712	36	1	0	7.513622	0.292529	1.875620
17	6	0	3.116679	1.697165	-0.051943	37	1	0	8.279664	-1.318851	1.868304
18	1	0	3.610051	2.659030	0.039444						

5. Photophysical Characteristics

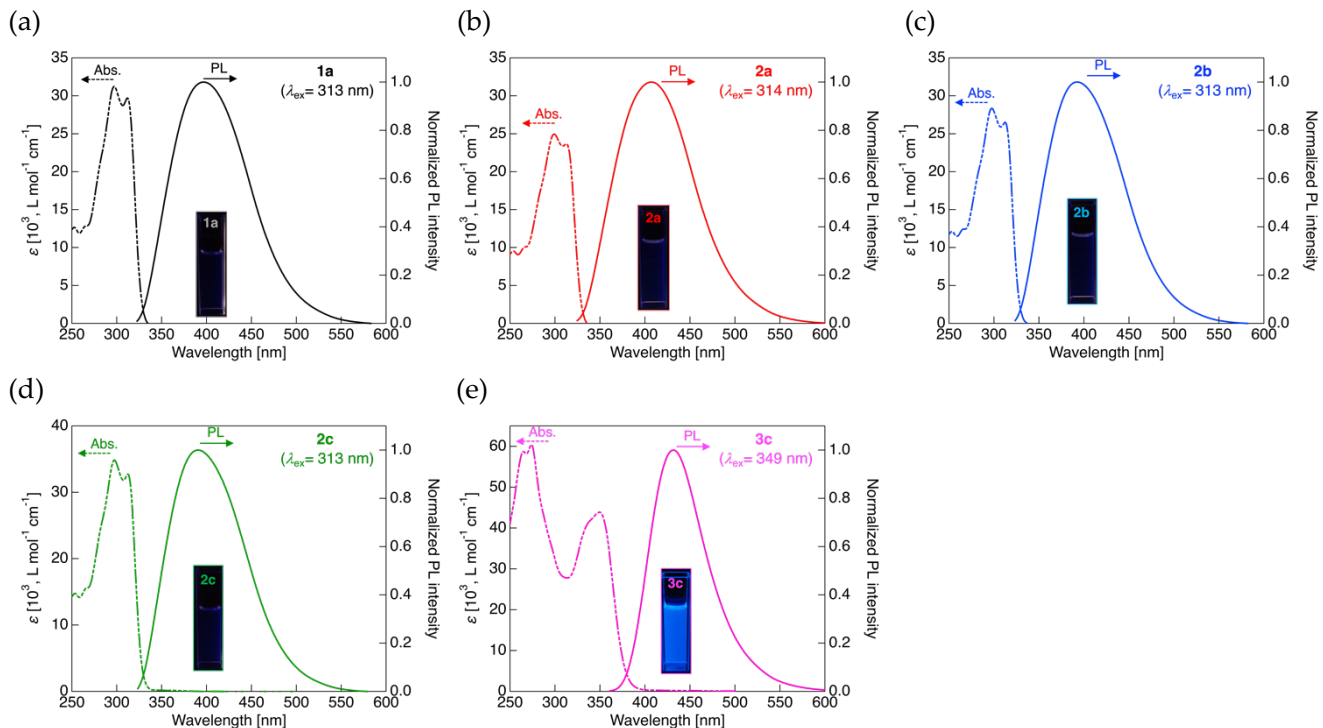


Figure S17. UV-vis and PL spectra of **1a**, **2a–c**, and **3c** in CH_2Cl_2 solution. Concentration: $1.0 \times 10^{-5} \text{ mol L}^{-1}$ for UV-vis and $1.0 \times 10^{-6} \text{ mol L}^{-1}$ for PL.

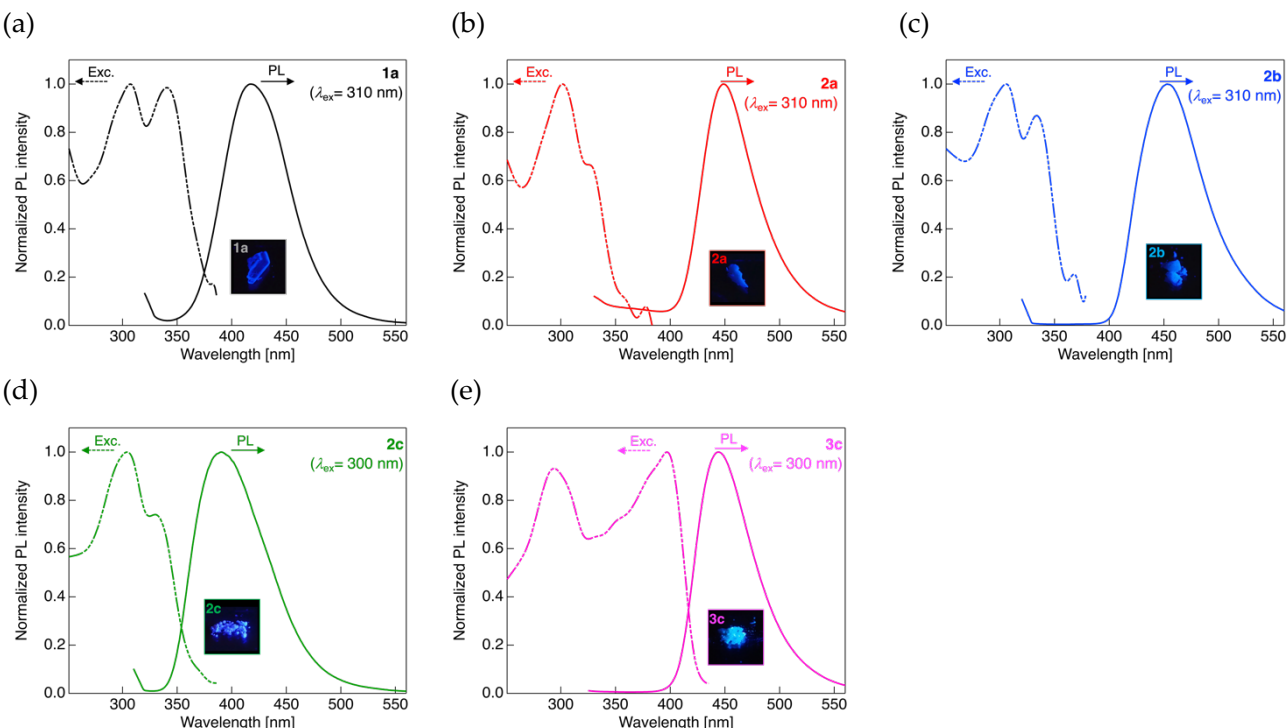


Figure S18. Excitation and PL spectra of **1a**, **2a–c**, and **3c** in crystalline state. Excitation spectra were obtained by monitoring PL at the maximum PL wavelength ($\lambda_{\text{em}} = 418 \text{ nm}$ for **1a**, 449 nm for **2a**, 453 nm for **2b**, 390 nm for **2c**, and 444 nm for **3c**).

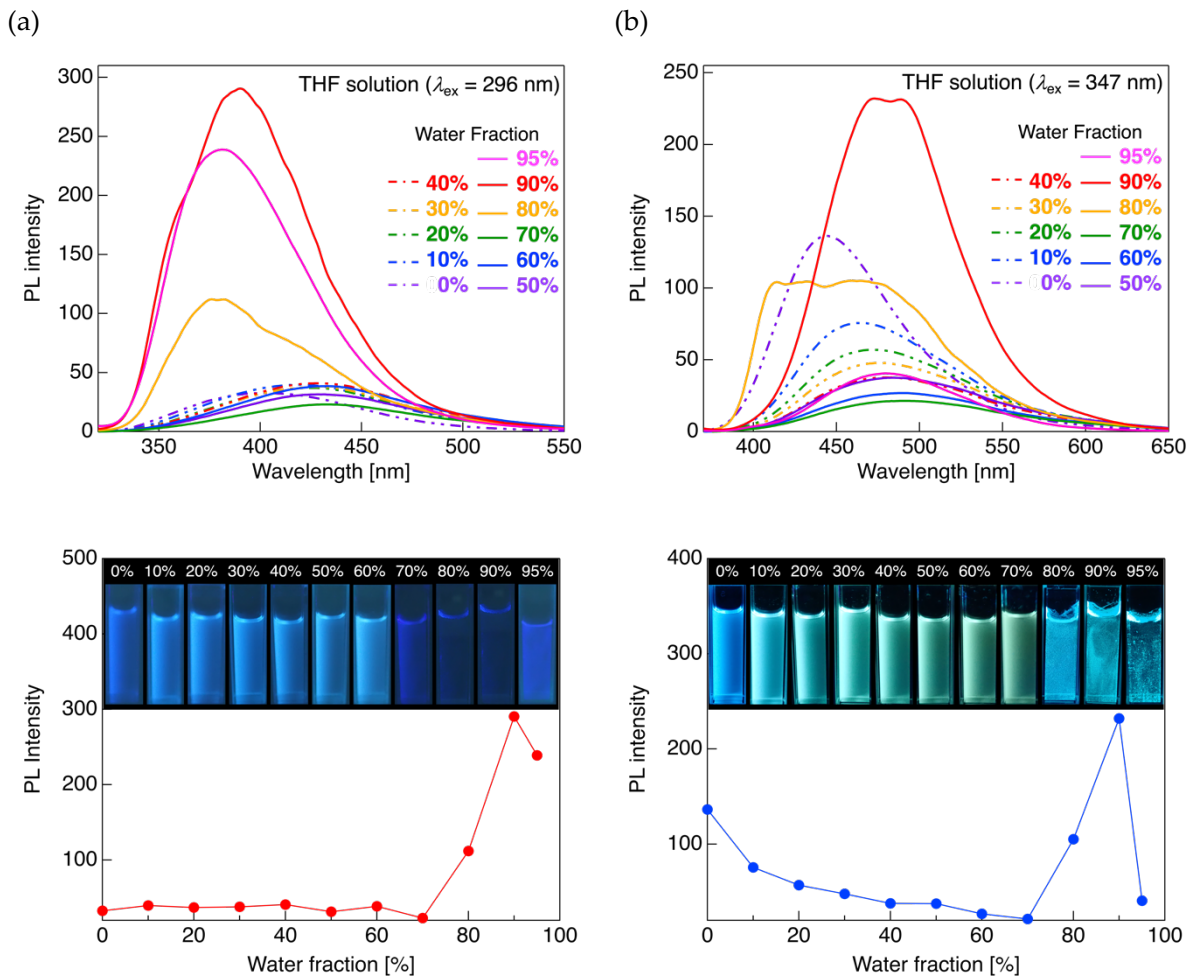


Figure S19. PL spectra and AIE characteristics of **2c** and **3c** in THF/H₂O mixed solvent system.

Table S9. Photophysical data of **2c** and **3c** in THF/H₂O mixed solvent system.

Water ratio [%]	2c ($\lambda_{\text{ex}} = 296 \text{ nm}$)		3c ($\lambda_{\text{ex}} = 347 \text{ nm}$)	
	λ_{PL} [nm]	PL intensity	λ_{PL} [nm]	PL intensity
0	402	32.56	444	136.37
10	419	39.69	462	75.60
20	423	37.01	473	56.90
30	428	37.87	476	47.81
40	430	40.93	480	37.73
50	429	31.47	485	37.52
60	433	38.53	490	26.84
70	434	23.00	493	21.40
80	382	111.91	459	105.14
90	390	290.50	473	232.03
95	381	238.89	479	40.55